

## SPOT14-Positive Neural Stem/Progenitor Cells in the Hippocampus Respond Dynamically to Neurogenic Regulators

Marlen Knobloch,<sup>1,2</sup> Carolin von Schoultz,<sup>1,2</sup> Luis Zurkirchen,<sup>1,2</sup> Simon M.G. Braun,<sup>1,2</sup> Mojca Vidmar,<sup>1</sup> and Sebastian Jessberger<sup>1,2,\*</sup>

<sup>1</sup>Brain Research Institute, Faculty of Medicine, University of Zurich, 8057 Zurich, Switzerland

<sup>2</sup>Neuroscience Center Zurich, University of Zurich and ETH Zurich, 8057 Zurich, Switzerland

\*Correspondence: [jessberger@hifo.uzh.ch](mailto:jessberger@hifo.uzh.ch)

<http://dx.doi.org/10.1016/j.stemcr.2014.08.013>

This is an open access article under the CC BY-NC-ND license (<http://creativecommons.org/licenses/by-nc-nd/3.0/>).

### SUMMARY

Proliferation of neural stem/progenitor cells (NSPCs) in the adult brain is tightly controlled to prevent exhaustion and to ensure proper neurogenesis. Several extrinsic stimuli affect NSPC regulation. However, the lack of unique markers led to controversial results regarding the in vivo behavior of NSPCs to different stimuli. We recently identified SPOT14, which controls NSPC proliferation through regulation of de novo lipogenesis, selectively in low-proliferating NSPCs. Whether SPOT14-expressing (SPOT14+) NSPCs react in vivo to neurogenic regulators is not known. We show that aging is accompanied by a marked disappearance of SPOT14+ NSPCs, whereas running, a positive neurogenic stimulus, increases proliferation of SPOT14+ NSPCs. Furthermore, transient depletion of highly proliferative cells recruits SPOT14+ NSPCs into the proliferative pool. Additionally, we have established endogenous SPOT14 protein staining, reflecting transgenic SPOT14-GFP expression. Thus, our data identify SPOT14 as a potent marker for adult NSPCs that react dynamically to positive and negative neurogenic regulators.

### INTRODUCTION

New neurons are generated throughout adulthood, and at least two neurogenic regions in the adult mammalian brain have been identified: the subventricular zone lining the lateral ventricles and the dentate gyrus (DG) of the hippocampal formation (Braun and Jessberger, 2014). It has been recently reported that in humans, up to one-third of hippocampal neurons are replaced with newborn neurons over a lifetime, implying a functional importance for this process (Spalding et al., 2013). There is increasing evidence that adult neurogenesis plays a role in cognitive processes, and aberrant or decreased levels of neurogenesis have been associated with a number of neuropsychiatric and neurodegenerative diseases (Braun and Jessberger, 2014; Christian et al., 2014). Notably, adult neurogenesis is dynamically regulated, and the control over the number of newly generated neurons occurs at multiple stages (Ma et al., 2009). For example, physical activity such as voluntary wheel running has a robust positive effect on the number of dividing cells in the DG, whereas an enriched environment has been shown to promote survival of newborn neurons (Ma et al., 2009). Aging, on the contrary, is accompanied by a drastic reduction in the number of dividing cells in the brain in rodents as well as in humans (Christian et al., 2014; Knoth et al., 2010).

However, the identification and in vivo tracking of neurogenic neural stem/progenitor cells (NSPCs) remains challenging, and no markers have been identified that

uniquely label NSPCs (Christian et al., 2014). The difficulties of identifying stem cells has led to controversial results, as studies assessing the in vivo behavior of NSPCs depend largely on the criteria and markers used (Bonaguidi et al., 2011; DeCarolis et al., 2013; Encinas et al., 2011; Lugert et al., 2010; Suh et al., 2007). Thus, it remains unclear whether distinct behaviors of NSPCs within the DG reflect different stem cell populations or whether the cells are just in a different state. Therefore, there is a need for novel and more specific markers to identify NSPCs in the adult hippocampus.

We have recently shown that SPOT14, a protein that is associated with lipid metabolic processes (Colbert et al., 2010; Cunningham et al., 1998), is specifically expressed in the subgranular zone (SGZ) of the DG in cells with radial and nonradial morphology, using GFP expression driven by the regulatory elements of the SPOT14 promoter (SPOT14 reporter mice). We have demonstrated that SPOT14+ cells are low-proliferating, neurogenic NSPCs, suggesting that SPOT14 could serve as a useful marker for NSPCs (Knobloch et al., 2013). However, the expression of endogenous SPOT14 protein and the response of SPOT14+ NSPCs to stimuli that influence neurogenesis remained unknown. Thus, we here established staining of endogenous SPOT14 to verify that SPOT14 reporter mice reflect endogenous protein expression and tested the effects of positive and negative regulators of neurogenesis on the behavior of SPOT14+ NSPCs in the adult hippocampus.

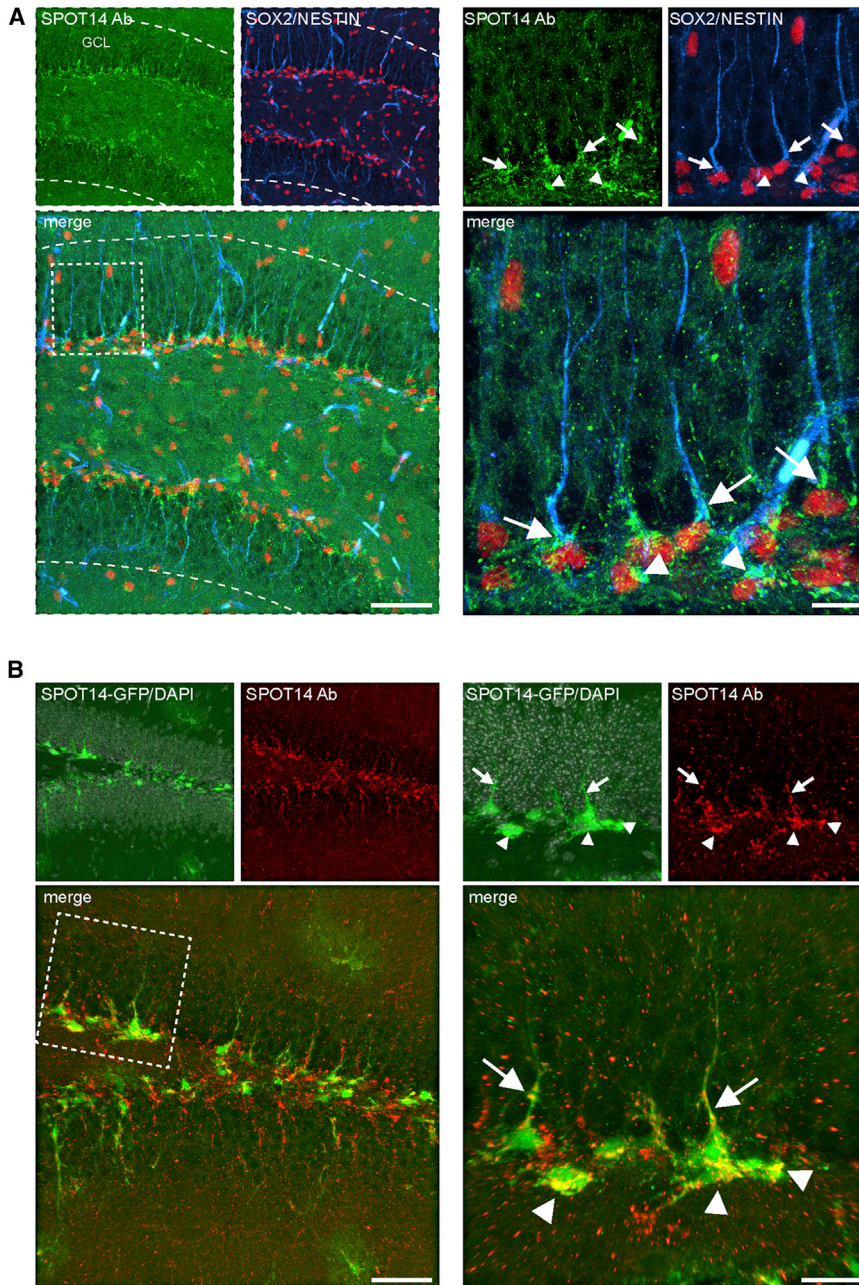


**Figure 1. Endogenous SPOT14 Protein Is Expressed in the Adult Hippocampus**

(A) Endogenous SPOT14 protein revealed by antibody staining is confined to the SGZ and colocalizes with the NSPC markers SOX2 (red) and NESTIN (blue). Shown are representative images of a wt mouse at 2 m (left panel) and a magnification of the boxed area (right panel). Arrows point to SPOT14/SOX2/NESTIN-positive radial NSPCs, and arrowheads point to SPOT14/SOX2-positive nonradial NSPCs.

(B) SPOT14-GFP-expressing cells colabel with the immunohistochemical signal from endogenous SPOT14 protein. Shown are representative images of a SPOT14 reporter mouse at 2 m (left panel) and a magnification of the boxed area (right panel). Arrows point to SPOT14-GFP/SPOT14-antibody positive radial NSPCs, and arrowheads point to SPOT14-GFP/SPOT14 antibody-positive nonradial NSPCs.

Scale bars represent 50  $\mu\text{m}$  (A and B, left) and 20  $\mu\text{m}$  (A and B, right). GCL, granular cell layer.

## RESULTS

### Endogenous SPOT14 Protein Is Expressed in Adult Hippocampal NSPCs

We have previously shown that transgenic expression of GFP driven by a bacterial artificial chromosome (BAC) containing the regulatory elements of the *Spot14* gene is highly restricted to hippocampal NSPCs (Knobloch et al., 2013). Whereas *Spot14* mRNA expression correlates with SPOT14-driven GFP (Knobloch et al., 2013), the expression

of endogenous SPOT14 protein remained unknown. By establishing an antibody staining against SPOT14, we found strong enrichment of the endogenous protein within the SGZ of the adult hippocampus (Figure 1A). Cellular phenotyping revealed that SPOT14-expressing cells show the morphological and molecular characteristics of adult hippocampal NSPCs, i.e., radial and nonradial morphology and expression of the previously described NSPC markers SOX2 and NESTIN (Figure 1A). Virtually all (97.5%  $\pm$  1.4% radial, 90.2%  $\pm$  1.3% nonradial)



SPOT14-GFP expressing cells colabeled with the immunohistochemical signal from endogenous SPOT14 protein (Figure 1B; Figure S1A available online). However, we found that a larger cohort of NSPCs expressed endogenous SPOT14 protein compared to SPOT14-GFP expression, suggesting that transgenic label expression is a reliable indicator of SPOT14 expression, albeit less efficient, similar to what has been described for other transgenic markers (Dhaliwal and Lagace, 2011).

### SPOT14+ NSPCs Disappear Markedly with Aging

We next assessed the in vivo behavior of SPOT14+ NSPCs to a negative regulator of neurogenesis. Neurogenesis is greatly reduced with aging, and this reduction is paralleled by the disappearance of putative NSPCs and/or decreased proliferation (Christian et al., 2014; Knoth et al., 2010). Whether or not SPOT14+ NSPCs disappear with aging is not known. We analyzed the expression of SPOT14-GFP at different time points in SPOT14 reporter mice. Postnatal day 7 (p7) and p21 mice as well as mice aged 2 months (2 m) and 7 months (7 m) showed consistent expression of the transgene within the DG (Figure 2A). However, there was a drastic reduction in the total number of SPOT14+ NSPCs with age, given the total number of GFP-positive cells at 2 m and 7 m (Figures 2A and 2B, left bars; Table S1). As SPOT14+ NSPCs exist both with and without radial processes (Knobloch et al., 2013), and because others have reported selective activation of nonradial cells upon extrinsic modulation of hippocampal neurogenesis (Bonaguidi et al., 2011; DeCarolis et al., 2013; Encinas et al., 2011; Kronenberg et al., 2003; Lugert et al., 2010; Suh et al., 2007), we further subdivided SPOT14+ cells according to their morphological difference into a radial and nonradial group (Figure 2B, middle bars; Table S1). This analysis showed that the decrease was dependent on a loss of both radial and nonradial cells. Consequently, the ratio of radial to nonradial NSPCs (Figure 2B, right bars; Table S1) was not significantly changed with age. To ensure that such substantial loss of SPOT14+ NSPCs with age is not due to changes in transgene expression in the SPOT14 reporter mouse, we performed in situ hybridizations using a riboprobe against *Spot14* mRNA. *Spot14* mRNA was consistently expressed in the SGZ of the DG and markedly decreased with aging (Figure 2C). Antibody staining against endogenous SPOT14 protein at p7, p21, 2 m, and 7 m further confirmed the marked decrease of SPOT14+ NSPCs with aging (Figure S1B). The overall morphology of SPOT14+ NSPCs as well as coexpression of other markers such as SOX2 and NESTIN did not change over time (Figure 2D), although NESTIN-positive processes in the granular zone of the DG were less detectable at 7 months. Taken together, these data show that

the number of both radial and nonradial SPOT14+ NSPCs decreases markedly with aging.

### Running Increases the Number of Proliferating SPOT14+ NSPCs

To address whether or not SPOT14+ NSPCs react to a positive regulator of adult neurogenesis, SPOT14 reporter mice had access to running wheels for 7 days. Consistent with previous reports, voluntary physical exercise led to a significant increase in the total number of proliferating cells in running mice compared to control mice, as measured by 5-ethynyl-2'-deoxyuridine (EdU) pulse labeling (Figures 3A and 3C; Table S2). The number of proliferating SPOT14+ NSPCs, which is low in control mice, increased significantly with running, indicating a mobilization of SPOT14+ NSPCs into the proliferating pool (Figures 3A and 3B; Table S2). Increased proliferation of SPOT14+ NSPCs upon running was reflected by a small but significant increase in the total number of SPOT14+ NSPCs in running versus control mice (Figure 3C; Table S2). We further subdivided the EdU+/SPOT14+ cells according to their morphological difference into radial and nonradial groups. The majority of double-positive cells in both running and control mice had nonradial morphology, and running did not change the ratio of proliferating radial to nonradial SPOT14+ NSPCs (Figure 3D; Table S2). Taken together, these data show that both radial and nonradial SPOT14+ NSPCs react with increased proliferation to running.

### Transient Depletion of Proliferative Cells Recruits SPOT14+ NSPCs

Given the dynamic behavior of SPOT14+ NSPCs to natural positive and negative regulators of neurogenesis, we artificially challenged the system by transient depletion of highly proliferative cells. We used the cytostatic drug temozolomide (TMZ) to selectively kill cycling cells and analyzed the number and proliferative activity of SPOT14+ NSPCs either directly after ablation or after 3 days of recovery using EdU pulse labeling. As expected, the treatment with TMZ reduced the proliferative cells in the DG of adult SPOT14 reporter mice compared to vehicle-injected control mice (Figures 4A and 4B; Table S3). Three days of recovery, however, was not enough time to reach the same amount of proliferating cells as before ablation. The total number of SPOT14+ cells was not changed upon treatment (Figures 4A and 4B; Table S3), in line with the fact that cytostatic drugs do mainly affect highly proliferating cells and that SPOT14+ NSPCs are low proliferating cells (Knobloch et al., 2013). However, as a consequence of the ablation, significantly more SPOT14+ cells were recruited into the proliferative pool 3 days after the end of TMZ treatment,

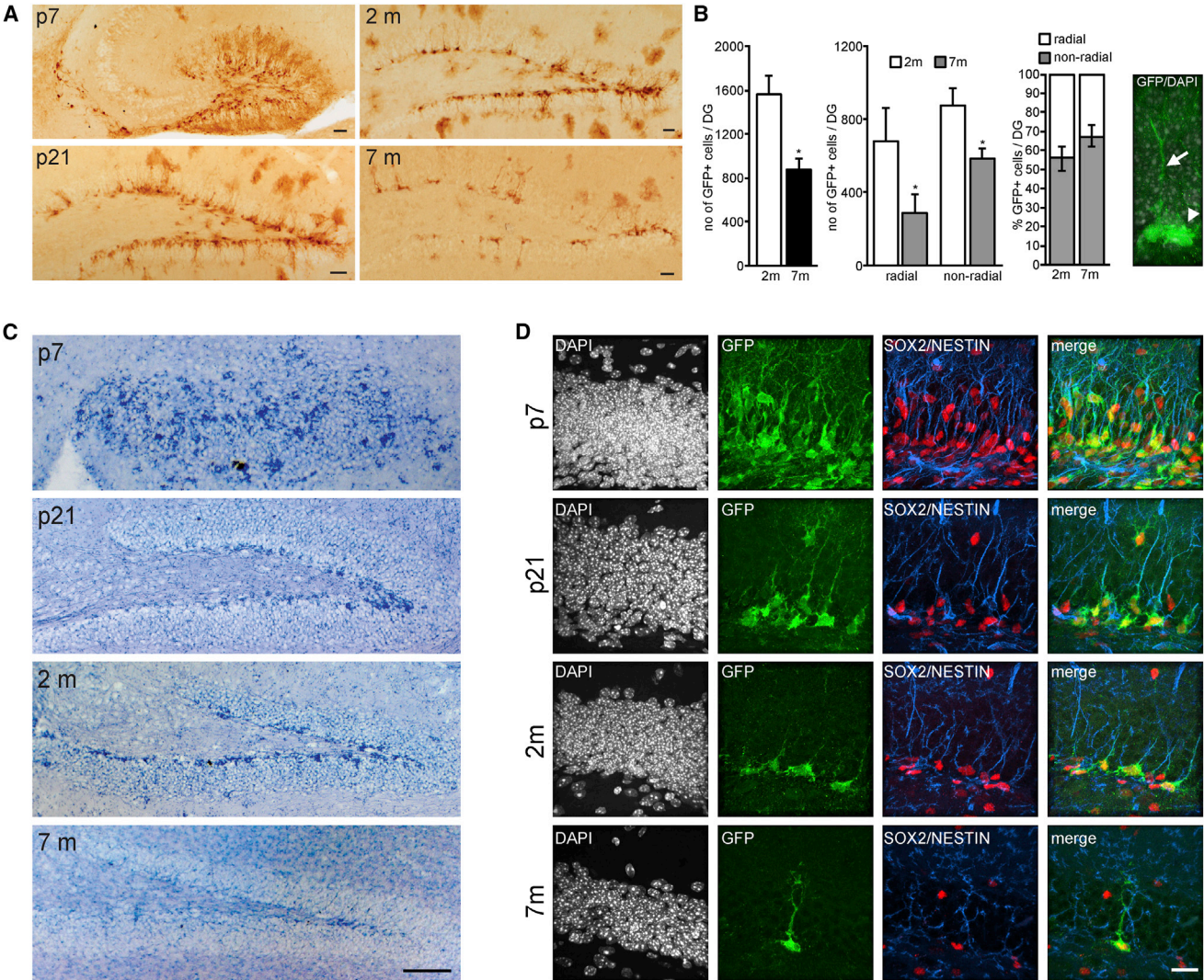


**Figure 2. The Number of SPOT14+ NSPCs Decreases with Aging**

(A) Analysis of SPOT14 reporter mice at postnatal day 7 (p7), day 21 (p21), 2 months (2 m), and 7 months (7 m) of age shows consistent expression of the transgene within the DG but robust reduction of SPOT14+ NSPCs with age. Shown are representative pictures of DAB stainings against GFP.

(B) Quantification of SPOT14+ NSPCs at 2 m (n = 4) and 7 m (n = 3) illustrating the substantial decrease in the total number of SPOT14+ cells with age (left bars). This decrease is dependent on a loss of both radial and nonradial cells (middle bars); thus, the ratio is not changed with age (right bars). An example image of a SPOT14+ radial (arrow) and nonradial (arrowhead) cell is shown on the right.

(C) In situ hybridization using a riboprobe against *Spot14* mRNA shows expression in the DG at p7, p21, 2 m, and 7 m. In parallel to the SPOT14-GFP expression shown in (A), *Spot14* mRNA is markedly decreasing with aging.

(D) Radial and nonradial morphology as well as expression of the NSPC markers SOX2 (red) and NESTIN (blue) in SPOT14+ cells (green) is present from early postnatal times through adulthood. Shown are representative images at p7, p21, 2 m, and 7 m.

Scale bars represent 100  $\mu$ m (A and C) and 20  $\mu$ m (D). Error bars represent mean  $\pm$  SEM. \*p < 0.05

an effect that started directly after the end of TMZ treatment (Figure 4C; Table S3). The majority of proliferating SPOT14+ NSPCs in all three groups had nonradial morphology, and TMZ treatment did not change the ratio of proliferating radial to nonradial SPOT14+

NSPCs (Figure 4D; Table S3). These data indicate that SPOT14+ NSPCs are reacting with increased proliferation upon transient ablation of highly proliferative cells, potentially to replenish the missing pool of cycling stem cells.

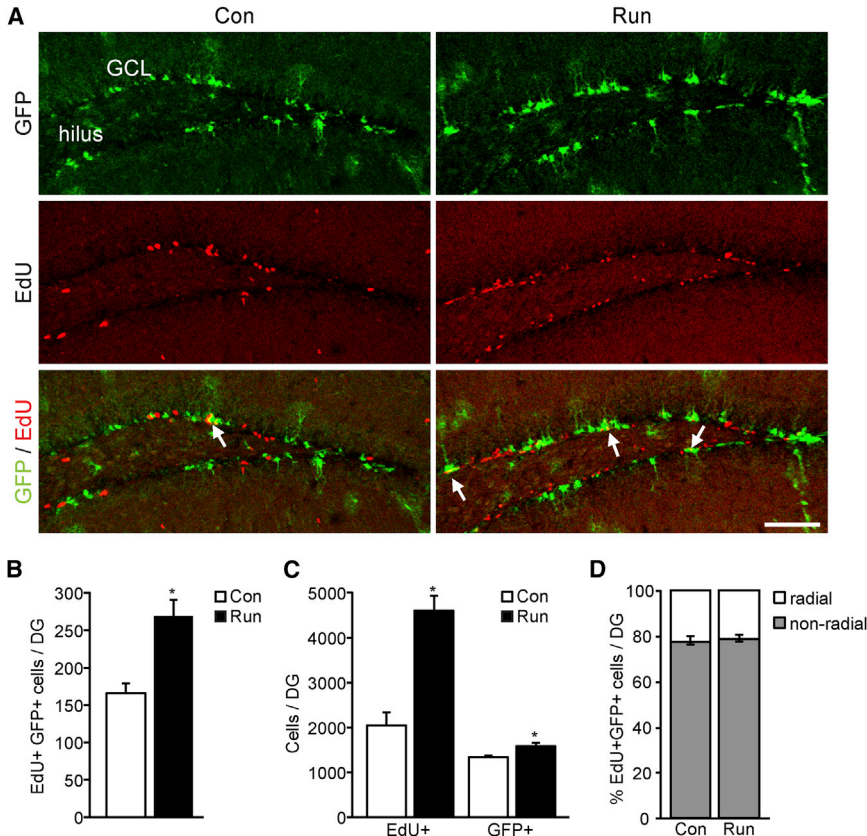


**Figure 3. Running Increases Proliferative Activity of SPOT14+ NSPCs**

(A) Running enhances proliferation in the DG, as measured by EdU pulse labeling, and leads to a mobilization of SPOT14+ NSPCs into the proliferative pool. Shown are representative confocal images of SPOT14 reporter mice with access to a running wheel (Run) and control mice (Con). Arrows point to GFP/EdU-colabeled cells. Top panels show single channels for SPOT14-GFP (green), middle panels EdU signal (red), and lower panels an overlay of SPOT14-GFP/EdU. (B) Quantification of SPOT14+/EdU+ double-labeled cells ( $n = 3$  per group). (C) Quantification of total numbers of EdU+ cells and SPOT14+ cells. Note the slight but significant increase in SPOT14+ NSPCs in running mice. (D) Quantification of SPOT14+/EdU+ cells subdivided into radial and nonradial morphology. The majority of double-positive cells in both running and control mice have nonradial morphology. Running does not change the ratio of proliferating radial to nonradial SPOT14+ NSPCs ( $n = 3$  per group). Scale bar represents 100  $\mu\text{m}$ . Error bars represent mean  $\pm$  SEM. \* $p < 0.05$

## DISCUSSION

One of the major problems in the field of adult neurogenesis is the in vivo identification of neurogenic, self-renewing NSPCs. So far, there are no unique markers that clearly label only NSPCs. Therefore, marker combinations together with morphological criteria are currently necessary to identify NSPCs. However, such combined measures render the in vivo labeling and fate tracking of NSPCs complicated. The identification of more restrictive markers will facilitate the isolation of NSPCs to enable gene and protein expression analyses of NSPCs without cross-contamination of other neural cell types and without the need for sophisticated multilabeling approaches (Becker-vordersandforth et al., 2014; Bracko et al., 2012; Pastrana et al., 2009).

We have recently shown that SPOT14 is expressed in a highly restrictive manner in low-proliferating NSPCs, making this protein an excellent candidate marker for adult hippocampal NSPCs (Knobloch et al., 2013). Even though SPOT14-GFP labels a small number of classical astrocytes in the molecular layer, its expression appears to be much more confined to neurogenic NSPCs compared to other transgenic markers such as NESTIN-GFP, highly expressed

in astrocytes in the DG and cornu ammonis/alveus or SOX2-GFP, highly expressed in the majority of hippocampal astrocytes (Bracko et al., 2012; Kronenberg et al., 2003; Suh et al., 2007).

To further establish the usefulness of SPOT14 as a NSPC marker, we established protocols allowing for immunohistochemical detection of endogenous SPOT14 protein. Comparing endogenous SPOT14 and transgenic SPOT14-GFP expression, we confirmed the reliability of the SPOT14 reporter mouse. Importantly, the availability of an antibody working on adult brain tissue sections substantially increases the usability of SPOT14 as a marker in combination with other antibodies or transgenic reporter mice.

Using the SPOT14-GFP expressing transgenic reporter line, we studied the behavior of SPOT14+ NSPCs in the DG to neurogenic regulators in vivo. Increased proliferative activity of SPOT14+ NSPCs upon running is in line with data from other transgenic reporter mice such as NESTIN-GFP mice (Kronenberg et al., 2003), SOX2-GFP mice (Suh et al., 2007), or HES5-GFP mice (Lugert et al., 2010). However, we did not observe a selective activation of radial NSPCs as shown in HES5-GFP mice (Lugert et al., 2010). SPOT14+ NSPCs rather behaved similarly to SOX2-GFP cells (Suh et al., 2007), where also both radial and nonradial

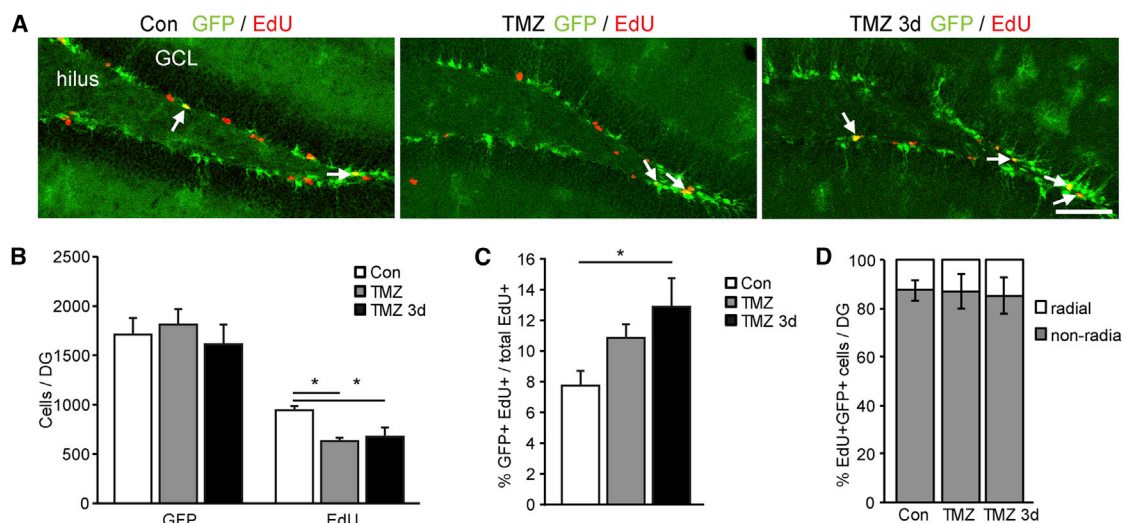


**Figure 4. Transient Ablation of Highly Proliferating Cells Recruits SPOT14+ NSPCs into the Proliferative Pool**

(A) Treatment with TMZ reduces the total number of proliferative cells in the DG of adult SPOT14 reporter mice. However, as a consequence of the ablation, more SPOT14+ cells are recruited into the proliferative pool. Shown are representative images (EdU in red, SPOT14-GFP in green) of control mice (left panel) and mice immediately or 3 days after TMZ (middle and right panel). Arrows point to GFP/EdU-colabeled cells.

(B) Quantifications show the drop in total EdU+ cells after TMZ treatment. The total number of SPOT14+ cells is not affected, in line with the fact that cytostatic drugs mainly affect highly proliferating cells (n = 3 per group).

(C) TMZ-induced transient depletion of highly proliferative cells recruits SPOT14+ cells into proliferation 3 days after the end of TMZ treatment.

(D) The majority of double-positive cells in all three groups have nonradial morphology and TMZ treatment does not change the ratio of proliferating radial to nonradial SPOT14+ NSPCs (n = 3 per group).

Scale bar represents 100  $\mu$ m. Error bars represent mean  $\pm$  SEM. \*p < 0.05

cell types increased proliferation upon running. This is supported by the finding that virtually all SPOT14+ NSPCs are also positive for SOX2 (Knobloch et al., 2013).

SPOT14 is functionally important by reducing substrate availability for fatty acid synthase (FASN), leading to reduced de novo lipogenesis (Knobloch et al., 2013). Interestingly, a recent publication demonstrated that *Fasn* mRNA is upregulated in the hippocampus upon running and that inhibition of FASN impaired exercise-mediated improvement in spatial memory, which was accompanied by reduced NSPC proliferation in the DG (Chorna et al., 2013). This further emphasizes the importance of de novo lipogenesis for proper neurogenesis and shows a dynamic regulation of this pathway upon an extrinsic stimulus.

To address whether SPOT14+ NSPCs also react to a negative regulator of neurogenesis, we analyzed the expression pattern of SPOT14 in the context of aging. Increased quiescence of NSPCs as well as a loss of NSPCs, decreased survival of progeny, or general negative influences of the aging systemic milieu have all been suggested to be the underlying cause of reduced production of new neurons with age (Couillard-Despres, 2012). The marked decrease of

SPOT14+ NSPCs with age supports the hypothesis that a loss of NSPCs occurs, but whether this is due to cell death or terminal differentiation is not clear (Encinas et al., 2011). However, our previous data with inducible SPOT14 lineage tracing in adult mice showed no increase in the amount of astrocytes 3 months after induction, suggesting that terminal differentiation of SPOT14+ NSPCs into astrocytes is not substantial (Knobloch et al., 2013).

NSPCs are not only influenced by physiological factors but also react to noxious stimuli. After ablation of the proliferative pool using antimetabolic drugs, a dynamic activation of quiescent adult NSPCs that fully re-establishes the germinal layer has been shown (Doetsch et al., 1999). The bona fide stem cells are not affected by the treatment, as they are not frequently dividing, but appear to perceive that there is need for regeneration and initiate proliferation. To test whether SPOT14+ NSPCs would respond similarly to such manipulation, we used the antimetabolic drug TMZ. TMZ treatment reduced proliferation by almost 30%, but 3 days of recovery was not enough to restore proliferation entirely. Nonetheless, the increase of proliferating SPOT14+ NSPCs became apparent immediately after drug treatment and reached significance 3 days later,



suggesting that these primarily quiescent cells can react to a noxious stimulus and contribute to regeneration. Both radial and nonradial SPOT14+ NSPCs increased their proliferation, speaking against SPOT14-labeled subpopulations that react distinctly to different stimuli, as described for HES5-GFP-positive stem cells (Lugert et al., 2010).

Taken together, we here show that the recently identified marker SPOT14 labels low-proliferating NSPCs in the hippocampus that react dynamically to positive and negative neurogenic stimuli *in vivo*. These data further validate the usefulness of this restrictive and functionally relevant marker to analyze the behavior of NSPCs to various extrinsic stimuli. The availability of functional SPOT14 antibodies, a SPOT14 reporter line, as well as an inducible SPOT14-CreER<sup>T2</sup> line (Knobloch et al., 2013) extend the current toolbox to study adult neurogenesis and will allow further dissection and better understanding of the complex regulation of NSPCs within the adult brain.

## EXPERIMENTAL PROCEDURES

### Animals

Animal experiments were approved by the veterinary office of the Canton of Zurich, Switzerland. The SPOT14 reporter mice were obtained as previously described (Knobloch et al., 2013). The running group ( $n = 3$ ) had free access to steel running wheels for 7 days. The control group ( $n = 3$ ) was kept single-caged in identical cages without running wheels. During days 4–7, all animals received four intraperitoneal (i.p.) injections of EdU (50 mg/kg, Sigma) and were killed 24 hr later. For the time-course analysis, three (p7, p21, 7 months) or four (2 months) SPOT14 reporter mice were perfused per age group. For the ablation experiment, SPOT14 reporter mice ( $n = 3$ ) received three i.p. injections of temozolomide (TMZ; Temodal, Schering-Plough, 25 mg/kg, in DMSO/PBS) or were control-injected with DMSO/PBS only ( $n = 3$ ). Two hours after the last injection, they received a single dose of EdU (50 mg/kg) and were killed 3 hr later. An additional group of mice ( $n = 3$ ) received TMZ as described above but was left to recover for 3 days. A single EdU injection was given 3 hr before perfusion. All mice were transcardially perfused with 0.9% saline followed by 4% paraformaldehyde (PFA)/0.1 M phosphate buffer. Brains were postfixed overnight in phosphate-buffered 4% PFA and subsequently stored in 30% sucrose-PBS solution.

### Tissue Preparation, Staining, and Image Analysis

Brains were processed and stained as previously described (Knobloch et al., 2013), and 40- $\mu\text{m}$ -thick free-floating serial sections were blocked with PBS containing 0.5% donkey serum and 0.05% Triton X-100 and stained with primary antibody in blocking solution overnight at 4°C. The GFP staining was additionally enhanced using biotinylated secondary antibodies followed by streptavidin-coupled fluorophores. Cell nuclei were counterstained with DAPI (1:5,000 in Tris-buffered saline, Sigma). Antibodies used were: rabbit  $\alpha$ -GFP (1:500, Invitrogen), chicken  $\alpha$ -GFP (1:500, Aves Labs), goat  $\alpha$ -SOX2 (1:500, Santa Cruz Biotech-

nology), and mouse  $\alpha$ -NESTIN (1:500, BD Biosciences). Secondary antibodies (Jackson ImmunoResearch or Chemicon International) were applied 1:250 at room temperature (RT) for 1–2 hr. For endogenous SPOT14 staining, sections were pretreated with PBS containing 0.5% donkey serum and 1% Triton X-100 for 5 hr at RT followed by 3 days primary antibody incubation in PBS containing 0.5% donkey serum and 0.05% Triton X-100 at 4°C (rabbit  $\alpha$ -SPOT14, 1:250, Abcam). The SPOT14 staining was additionally enhanced using a biotinylated secondary antibody (2–4 hr RT) followed by streptavidin-coupled fluorophores (2–4 hr RT). 3,3'-Diaminobenzidine (DAB) staining was done as described above with quenching of endogenous peroxidase in 0.6% H<sub>2</sub>O<sub>2</sub> prior to antibody incubation. The Vectastain ABC Kit was used for the color reaction according to the manufacturer's protocol (Vectastain ABC Kit, Vector Laboratories). EdU stainings were performed before antibody incubation using the Click-iT EdU Imaging Kit (Invitrogen). Every 12<sup>th</sup> or every 4<sup>th</sup> section (corresponding to a 12<sup>th</sup> or to a 3<sup>rd</sup> of the entire brain) of coronally or sagittally cut brains spanning the complete rostrocaudal extent of the hippocampus were collected and used for quantifications, and 20- $\mu\text{m}$ -thick image stacks of DGs were taken with a confocal microscope (Leica SP2-AOBS and Zeiss LSM700). Shown are maximum intensity projections. DAB staining was analyzed using a Zeiss AxioImager microscope. GFP-expressing cells with apical processes spanning the granule cell layer were classified as radial glia-like cells and GFP-expressing cells with short, horizontal processes were classified as nonradial glia-like cells, as described previously (Kronenberg et al., 2003; Lugert et al., 2010; Suh et al., 2007). The number of EdU- and GFP-positive cells was counted in a blinded manner using Imaris (Bitplane) 3D reconstructions to verify signal colocalization for double-positive cells.

### Statistical Analysis

Unpaired *t* tests and nonparametric Mann-Whitney *U* tests were used for the running and aging analyses. Differences in the three groups of the TMZ ablation experiment were analyzed using ANOVA followed by Fisher's post hoc test. Numbers (*n*) indicate the number of individual mice. Significance levels were set at  $p < 0.05$ .

## SUPPLEMENTAL INFORMATION

Supplemental Information includes one figure and three tables and can be found with this article online at <http://dx.doi.org/10.1016/j.stemcr.2014.08.013>.

## AUTHOR CONTRIBUTIONS

M.K. contributed to the concept, designed and performed experiments, analyzed data, and wrote the paper. C.v.S. performed experiments and analyzed data. L.Z., S.M.G.B., and M.V. contributed to the running experiment. S.J. developed the concept, designed experiments, and wrote the paper.

## ACKNOWLEDGMENTS

We thank Irmgard Amrein for providing running wheels and Ghazaleh Tabatabai for experimental advice on the TMZ experiments. This study was supported by the NCCR Neural Plasticity and



Repair, Swiss National Science Foundation, Zurich Neuroscience Center, Novartis, and the Theodore Ott and Janggen-Pöhn foundations. C.v.S. is supported by a Boehringer Ingelheim Fonds fellowship.

Received: April 12, 2014

Revised: August 21, 2014

Accepted: August 21, 2014

Published: September 25, 2014

## REFERENCES

- Beckervordersandforth, R., Deshpande, A., Schäffner, I., Huttner, H.B., Lepier, A., Lie, D.C., and Götz, M. (2014). In vivo targeting of adult neural stem cells in the dentate gyrus by a split-Cre approach. *Stem Cell Reports* 2, 153–162.
- Bonaguidi, M.A., Wheeler, M.A., Shapiro, J.S., Stadel, R.P., Sun, G.J., Ming, G.-L., and Song, H. (2011). In vivo clonal analysis reveals self-renewing and multipotent adult neural stem cell characteristics. *Cell* 145, 1142–1155.
- Bracko, O., Singer, T., Aigner, S., Knobloch, M., Winner, B., Ray, J., Clemenson, G.D., Jr., Suh, H., Couillard-Despres, S., Aigner, L., et al. (2012). Gene expression profiling of neural stem cells and their neuronal progeny reveals IGF2 as a regulator of adult hippocampal neurogenesis. *J. Neurosci.* 32, 3376–3387.
- Braun, S.M.G., and Jessberger, S. (2014). Adult neurogenesis: mechanisms and functional significance. *Development* 141, 1983–1986.
- Chorna, N.E., Santos-Soto, I.J., Carballeira, N.M., Morales, J.L., de la Nuez, J., Cátala-Valentin, A., Chorny, A.P., Vázquez-Montes, A., and De Ortiz, S.P. (2013). Fatty acid synthase as a factor required for exercise-induced cognitive enhancement and dentate gyrus cellular proliferation. *PLoS One* 8, e77845.
- Christian, K.M., Song, H., and Ming, G.-L. (2014). Functions and dysfunctions of adult hippocampal neurogenesis. *Annu. Rev. Neurosci.* 37, 243–262.
- Colbert, C.L., Kim, C.-W., Moon, Y.-A., Henry, L., Palnitkar, M., McKean, W.B., Fitzgerald, K., Deisenhofer, J., Horton, J.D., and Kwon, H.J. (2010). Crystal structure of Spot 14, a modulator of fatty acid synthesis. *Proc. Natl. Acad. Sci. USA* 107, 18820–18825.
- Couillard-Despres, S. (2012). Hippocampal neurogenesis and ageing. In *Current Topics in Behavioral Neurosciences*, M.A. Geyer, B.A. Ellenbroek, and C.A. Marsden, eds. (Berlin, Heidelberg: Springer Berlin Heidelberg), pp. 343–355.
- Cunningham, B.A., Moncur, J.T., Huntington, J.T., and Kinlaw, W.B. (1998). “Spot 14” protein: a metabolic integrator in normal and neoplastic cells. *Thyroid* 8, 815–825.
- DeCarolis, N.A., Mechanic, M., Petrik, D., Carlton, A., Ables, J.L., Malhotra, S., Bachoo, R., Götz, M., Lagace, D.C., and Eisch, A.J. (2013). In vivo contribution of nestin- and GLAST-lineage cells to adult hippocampal neurogenesis. *Hippocampus* 23, 708–719.
- Dhaliwal, J., and Lagace, D.C. (2011). Visualization and genetic manipulation of adult neurogenesis using transgenic mice. *Eur. J. Neurosci.* 33, 1025–1036.
- Doetsch, F., García-Verdugo, J.M., and Alvarez-Buylla, A. (1999). Regeneration of a germinal layer in the adult mammalian brain. *Proc. Natl. Acad. Sci. USA* 96, 11619–11624.
- Encinas, J.M., Michurina, T.V., Peunova, N., Park, J.-H., Tordo, J., Peterson, D.A., Fishell, G., Koulikov, A., and Enikolopov, G. (2011). Division-coupled astrocytic differentiation and age-related depletion of neural stem cells in the adult hippocampus. *Cell Stem Cell* 8, 566–579.
- Knobloch, M., Braun, S.M.G., Zurkirchen, L., von Schoultz, C., Zamboni, N., Araúzo-Bravo, M.J., Kovacs, W.J., Karalay, O., Suter, U., Machado, R.A., et al. (2013). Metabolic control of adult neural stem cell activity by Fasn-dependent lipogenesis. *Nature* 493, 226–230.
- Knoth, R., Singec, I., Ditter, M., Pantazis, G., Capetian, P., Meyer, R.P., Horvat, V., Volk, B., and Kempermann, G. (2010). Murine features of neurogenesis in the human hippocampus across the lifespan from 0 to 100 years. *PLoS ONE* 5, e8809.
- Kronenberg, G., Reuter, K., Steiner, B., Brandt, M.D., Jessberger, S., Yamaguchi, M., and Kempermann, G. (2003). Subpopulations of proliferating cells of the adult hippocampus respond differently to physiologic neurogenic stimuli. *J. Comp. Neurol.* 467, 455–463.
- Lugert, S., Basak, O., Knuckles, P., Haussler, U., Fabel, K., Götz, M., Haas, C.A., Kempermann, G., Taylor, V., and Giachino, C. (2010). Quiescent and active hippocampal neural stem cells with distinct morphologies respond selectively to physiological and pathological stimuli and aging. *Cell Stem Cell* 6, 445–456.
- Ma, D.K., Kim, W.R., Ming, G.-L., and Song, H. (2009). Activity-dependent extrinsic regulation of adult olfactory bulb and hippocampal neurogenesis. *Ann. N Y Acad. Sci.* 1170, 664–673.
- Pastrana, E., Cheng, L.-C., and Doetsch, F. (2009). Simultaneous prospective purification of adult subventricular zone neural stem cells and their progeny. *Proc. Natl. Acad. Sci. USA* 106, 6387–6392.
- Spalding, K.L., Bergmann, O., Alkass, K., Bernard, S., Salehpour, M., Huttner, H.B., Boström, E., Westerlund, I., Vial, C., Buchholz, B.A., et al. (2013). Dynamics of hippocampal neurogenesis in adult humans. *Cell* 153, 1219–1227.
- Suh, H., Consiglio, A., Ray, J., Sawai, T., D’Amour, K.A., and Gage, F.H. (2007). In vivo fate analysis reveals the multipotent and self-renewal capacities of Sox2+ neural stem cells in the adult hippocampus. *Cell Stem Cell* 1, 515–528.

**Stem Cell Reports, Volume 3**

**Supplemental Information**

**SPOT14-Positive Neural Stem/Progenitor Cells in the  
Hippocampus Respond Dynamically to Neurogenic  
Regulators**

**Marlen Knobloch, Carolin von Schoultz, Luis Zurkirchen, Simon M.G. Braun, Mojca Vidmar, and Sebastian Jessberger**

**Figure S1**

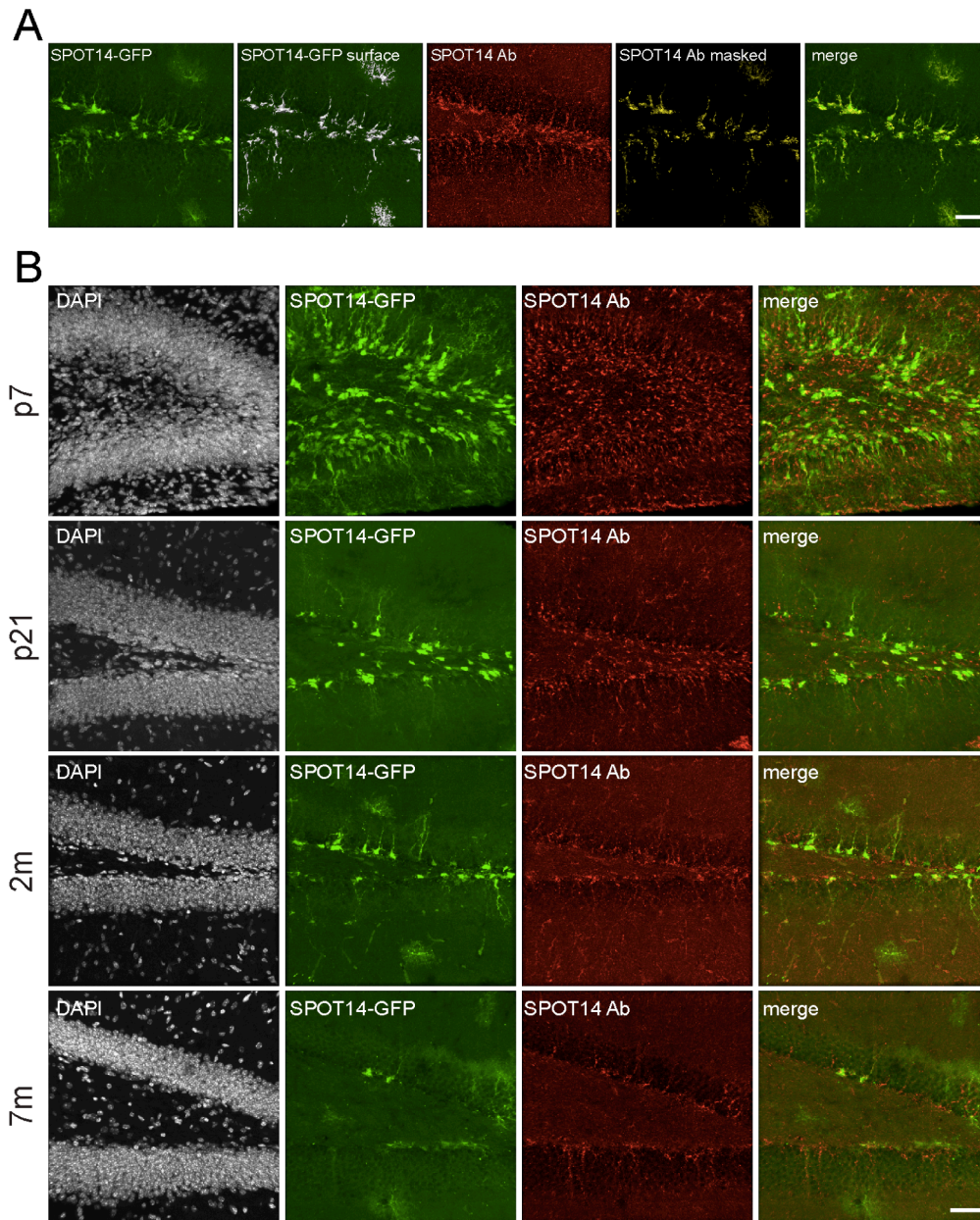


**Figure S1. Endogenous SPOT14 protein is expressed by SPOT14-GFP positive NSPCs**

(A) Quantification method to analyze co-labeling of SPOT14-GFP and endogenous SPOT14 immunohistochemical signal: a 3D surface of the GFP signal is generated using Imaris software (first and second panel), the surface is then used on the endogenous SPOT14 signal (third panel) to mask this channel and generate an artificial co-labeling channel (fourth panel). This co-labeling channel is used together with the SPOT14-GFP channel to determine the number of positive radial and non-radial NSPCs positive for both reporter and endogenous SPOT14. Scale bar represents 50  $\mu$ m.

(B) Analysis of SPOT14 reporter mice at postnatal day 7 (p7), day 21 (p21), 2 months (2m) and 7 months (7m) of age shows that both the endogenous SPOT14 and the SPOT14-GFP reporter signals are drastically reduced with age. Scale bar represents 50  $\mu$ m.

**Table S1: detailed cell numbers of aging experiment**

<b>Aging (Figure 2)</b>	2m (n = 4) (mean ± SEM)	7m (n = 3) (mean ± SEM)
Total number of SPOT14+ cells per DG	1557 ± 176	876 ± 98
Total number of radial SPOT14+ cells per DG	682 ± 97	288 ± 50
Total number of non-radial SPOT14+ cells per DG	875 ± 82	588 ± 61
Percentage of radial SPOT14+ cells per DG	43.8 ± 6.3	32.9 ± 5.7
Percentage of non-radial SPOT14+ cells per DG	56.2 ± 5.3	67.1 ± 7.0

**Table S2: detailed cell numbers of running experiment**

<b>Running (Figure 3)</b>	Con (n = 3) (mean ± SEM)	Run (n = 3) (mean ± SEM)
Total number of EdU+ cells per DG	2052 ± 287.7	4605 ± 325.1
Total number of SPOT14+ / EdU+ double positive cells per DG	166 ± 13.2	269 ± 21.5
Total number of SPOT14+ cells per DG	1338 ± 32.4	1584 ± 75.3
Percentage of radial SPOT14+ / EdU+ double positive cells per DG	22.6 ± 2.4	21.4 ± 1.8
Percentage of non-radial SPOT14+ / EdU+ double positive cells per DG	77.4 ± 2.4	78.6 ± 1.8

**Table S3: detailed cell numbers of transient ablation experiment**

<b>Transient ablation (Figure 4)</b>	Con (n = 3) (mean ± SEM)	TMZ (n = 3) (mean ± SEM)	TMZ 3d (n = 3) (mean ± SEM)
Total number of EdU+ cells per DG	943.5 ± 42.7	632.0 ± 31.4	678.0 ± 90.8
Total number of SPOT14+ cells per DG	1708.5 ± 171.6	1810.0 ± 158.5	1612.0 ± 199.4
Percentage of SPOT14+ / EdU+ double positive cells of all EdU+ cells	7.7 ± 0.9	10.8 ± 0.8	12.8 ± 1.8
Percentage of radial SPOT14+ / EdU+ double positive cells per DG	12.6 ± 4.2	12.8 ± 7.2	14.7 ± 7.4
Percentage of non-radial SPOT14+ / EdU+ double positive cells per DG	87.4 ± 4.2	87.2 ± 7.2	85.3 ± 7.4